Effect of iron additions on intergranular cohesion in chromium

2009 J. Phys.: Condens. Matter 21 485002

(http://iopscience.iop.org/0953-8984/21/48/485002)

J. Phys.: Condens. Matter **21** (2009) 485002 (8pp) doi:10.1088/0953-8984/21/48/485002

Effect of iron additions on intergranular cohesion in chromium

T Ossowski, E Wachowicz and A Kiejna

Institute of Experimental Physics and Interdisciplinary Centre for Materials Modeling, University of Wrocław, Plac M Borna 9, PL-50-204 Wrocław, Poland

E-mail: kiejna@ifd.uni.wroc.pl

Received 26 June 2009, in final form 4 September 2009
Published 30 October 2009
Online at stacks.iop.org/JPhysCM/21/485002

Abstract

The structural, cohesive, and magnetic properties of (111) and (210) tilt grain boundaries (GBs) in pure Cr, and in Cr with Fe additions, are studied from first principles. Different concentration and position of solute atoms are considered. Our calculations show that Fe atoms placed in the GB interstice enhance cohesion, whereas Fe substituted for one of the Cr layer atoms, in most cases, has very small (or negligible) effect on the cohesion at GBs in Cr. We have found that Fe additions show a tendency to enrich the boundaries in Cr. In the presence of Fe additions the magnetic moments on the GB host atoms are substantially modified and those on Fe impurities are reduced. In most cases the moments on Fe additions remain much higher than the local moments on the Cr atoms.

(Some figures in this article are in colour only in the electronic version)

1. Introduction

A high melting point and its wear and corrosion resistance mean that chromium is widely used as a protective coating on steels. Thin Cr layers electro-deposited on steels adhere strongly to the support but usually they show micro-cracks. With exposure to high temperature the micro-cracks propagate through the chromium [1], allowing the reactive gases to penetrate through the Cr layer and corrode the steel. Thus, in order to reduce the crack formation it is important to study the different factors which influence the mechanical strength at the boundaries of small Cr crystallites. In general the mechanical properties of polycrystalline metals depend on the cohesion at bulk interfaces between the crystal grains. Foreign atom additions modify cohesive properties of the host metal. By segregating to the boundaries impurity atoms may enrich the boundary region of the pure metal crystallite, thus affecting the structure and chemistry of interfaces, and consequently their mechanical properties. This effect is manifested in the intergranular embrittlement (decohesion) or strengthening of the material. At room temperature pure chromium is brittle and addition of Fe atoms may make it ductile. In this work we explore the effect of a small amount of Fe addition on the cohesive and mechanical properties of GBs in chromium. Fe atoms introduced to chromium, and vice versa, form a solid solution whose properties are affected in a complex way by the magnetism in both constituting elements. Ferromagnetic (FM) Fe atoms have a huge magnetic moment in comparison to that on the antiferromagnetic (AFM) bulk Cr atoms and the alloy is FM to quite low concentrations of iron. The interplay between magnetism and structure in both constituents depends on different structural settings. The FeCr alloys with small Cr content have useful engineering properties and applications which stimulate a lot of current experimental and theoretical research. First principles calculations based on the density functional theory (DFT) have been extensively used to study structural properties and to describe the electronic structure effects, such as competition between ferro- and antiferromagnetism in the alloy, the mixing behaviour and the heat of formation of various FeCr bulk-alloy structures with small Cr contents [2–5]. The properties of CrFe alloys with small Fe concentration are relatively unexplored. The electronic structure and magnetic properties of solute Fe in bulk AFM Cr were discussed in [6–9]. However, in contrast to numerous first principles studies of intergranular cohesion in pure and doped iron, which were initiated almost twenty years ago [10–17], *ab initio* calculations for Cr surfaces and interfaces are very seldom treated [18–20]. To the best of our knowledge no such studies were reported dealing with the interface properties of dilute CrFe alloys with high Cr contents.

In this work we apply first principles DFT calculations in order to obtain reliable quantitative information on the structure, energetics, and magnetism of Cr interfaces on an electronic level. We address the effect of a low concentration

(below 6 at.%) of Fe additions to the Cr-host grains on the GB cohesion. Our calculations allow us to gain insight into the microstructure and bonding at GBs in Cr and their dependence on electronic and magnetic properties modified by a small amount of Fe. Furthermore, we show that these calculations are able to predict segregation of Fe additions at the GBs in Cr. Two different symmetric tilt GBs were chosen for the model system to study anisotropy of GB properties in order to understand the relation between the interfacial structure of the GBs and the reduced coordination of their atoms, and the electronic and magnetic properties of the systems. The results of this work allow a comparison with the corresponding results for same GBs in iron [21] and altogether give a more complete picture of the GB properties in the FeCr alloy, viewed from the two ending points of the phase diagram.

The rest of the paper is organized as follows: in section 2 we describe briefly the computational methods and details of calculations. We begin section 3 with the presentation and discussion of our results for the GBs in pure Cr, and continue with a comparison and discussion of the effect of Fe additions. Section 4 presents a summary.

2. Method of calculations

We performed total energy calculations based on the density functional theory with the generalized gradient approximation (GGA) applied to the exchange–correlation energy functional [22] as implemented in the VASP code [23, 24]. The solutions of the Kohn–Sham equations were represented in a plane-wave basis set with a kinetic-energy cutoff of 350 eV. The electron–ionic core interactions were described by the projector-augmented-wave (PAW) potentials [25, 26]. The calculational slabs were constructed using the theoretical equilibrium lattice parameter (a = 2.841 Å) for bcc Cr, determined by us previously [20] in good agreement with experiment (a_{exp} = 2.88 Å), and other calculations. The (111) or (210) oriented slabs representing the respective Cr grains, each of 18 and 20 Cr atomic layers, were mirrored with respect to the outer lattice plane (figure 1) to form the 70.5° Σ3(111) and 53.1° Σ5(210) tilt GB slabs of 36 and 40 Cr layers, respectively. The system was repeated periodically throughout space thus forming two antiparallel oriented GBs per supercell. In the coincidence site lattice model notation [27], applied throughout this work Σ3 and Σ5 mean that one in three, and one in five lattice points, respectively, of the pairs of two tilted (111) and (210) surfaces are coincident. In AFM Cr the initial magnetic moments on atoms of the two grains are parallel within layer, but are antiparallel to those on the neighbouring layer atoms in the direction perpendicular to boundary plane. The volume and shape of the supercell were relaxed, and the positions of all atoms were optimized until the forces on each atom were below 0.05 eV Å^{-1}. The Brillouin zone of the Σ3(111) and Σ5(210) slabs was sampled using respectively 8 × 8 × 1 and 4 × 8 × 1 grids of special k-points [28]. The point groups associated with the full space groups of the respective slabs are D_{6h} and C_{2h}. To calculate the fractional occupancies the first order Methfessel–Paxton [29] method of the Fermi surface smearing was applied

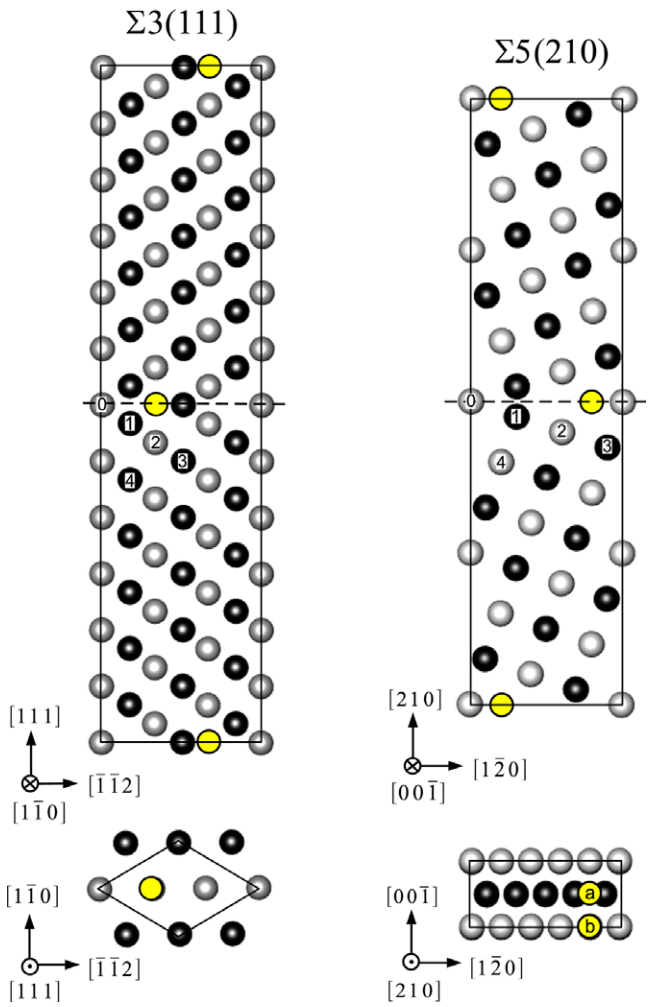

Figure 1. Side view of the supercells applied in the calculations representing the Σ3(111) and Σ5(210) boundaries between bcc Cr grains. The lighter and darker balls mark the atoms belonging to two different planes. The atoms of two subsequent layers, both in the figure plane and parallel to the GB plane are stacked antiferromagnetically. The yellow (open) circles indicate positions in the GB interstice where Fe atoms were placed. The numbers on atoms label the substitutional positions in different grain layers. In the lower panels top views of the supercells are shown, viewed in the cross-section plane passing through the GB (broken line). The atoms of the three and ten topmost layers of Σ3 and Σ5 GB are visible, respectively. The 'a' and 'b' on the Σ5 top view panel label two different interstitial sites.

with a width of 0.2 eV. The free surfaces (FSs) of (111) or (210) type, which were needed for further calculations, were created by using slabs of 18 and 20 Cr layers that remained after removal from the relaxed GB supercell of the second grain. Such a slab plus the vacuum region left by the removed grain was repeated periodically in space. For the FS slabs only the positions of atoms were relaxed while both the size and shape of the supercell were adopted from the GB slab.

In discussing the cohesive properties of GBs, and their comparison with the cohesion in an ideal crystal, it is useful to define the grain boundary energy

$$\gamma_{\mathrm{GB}} = E_{\mathrm{GB}} - nE_{\mathrm{atom}}^{\mathrm{bulk}}, \qquad (1)$$

where E_{GB} is the total energy of the grains at the equilibrium separation and E_{atom}^{bulk} is the energy per atom of the ideal bulk crystal of n atoms.

An important quantity which is useful in analysing the role of impurity atoms in the energetics of the cohesive and mechanical properties of GBs, based on a thermodynamic approach developed by Rice and Wang [30], is the formation energy, defined as

$$\gamma_f = E_{GB} - 2E_{FS}, \tag{2}$$

where $2E_{FS}$ represents the total energy of two (infinitely separated) free surfaces which form the GB, taking into account all relaxation processes. The GB formation energy (the work of separation) is equivalent to the adhesive bonding energy and thus for two identical grains in full registry is (negative of) twice the surface energy.

The key quantity that determines the strengthening or embrittling effect of an impurity is the strengthening energy ΔE_{SE} which can be expressed [15, 21] as

$$\Delta E_{SE} = \gamma_f^{imp} - \gamma_f^{cln}, \tag{3}$$

where γ_f^{imp} is the formation energy of the GB with an impurity, and γ_f^{cln} is the formation energy of a GB in pure metal [21]. The positive/negative ΔE_{SE} means that the impurity weakens/strengthens the GB.

A weakening/strengthening of a GB due to the presence of impurities is considered by different authors as caused either by changes in the chemical bonding, due to the electronic charge redistribution, or by a structural size effect connected with a mechanical distortion of the system. There is no perfect way to separate these two effects and in this work we adopt the method proposed by Lozovoi *et al* [31]. In this approach, by analysing different energetic contributions to the binding energy of a substitutional impurity one can discriminate the *chemical*, *mechanical*, and *host removal* energy components [21, 31]. The first of them results from a direct interaction between an impurity and the host atoms, and is defined as the difference between the formation energy of a GB with impurity γ_f^{imp} and γ_f^{frz} which is the formation energy of GB with removed impurity while keeping all the host atoms in frozen positions. The mechanical contribution is given by the energy release due to relaxation of the host atoms, after the impurity is removed, and can be written as the difference between γ_f^{frz} and the $\gamma_f^{sub/frz}$, which represent the formation energies calculated for the clean GB frozen in the relaxed configuration, and with a removed host atom subsequently replaced by an impurity (for an interstitial impurity). Finally, for substitutional impurity there is an energy change due to the removal of a host atom which can be calculated as the difference between $\gamma_f^{sub/frz}$ and γ_f^{cln}.

The segregation energy (enthalpy) of the solute Fe atom at the host GB was calculated as the following total energy difference

$$E_{segr} = E_{Fe,GB} - E_{Fe,bulk}, \tag{4}$$

where $E_{Fe,GB}$ and $E_{Fe,bulk}$ are total energies of the slab with one of the Cr atoms, respectively at the GB or in the bulk, substituted by the Fe. The negative E_{segr} means that the impurity segregates at the GB.

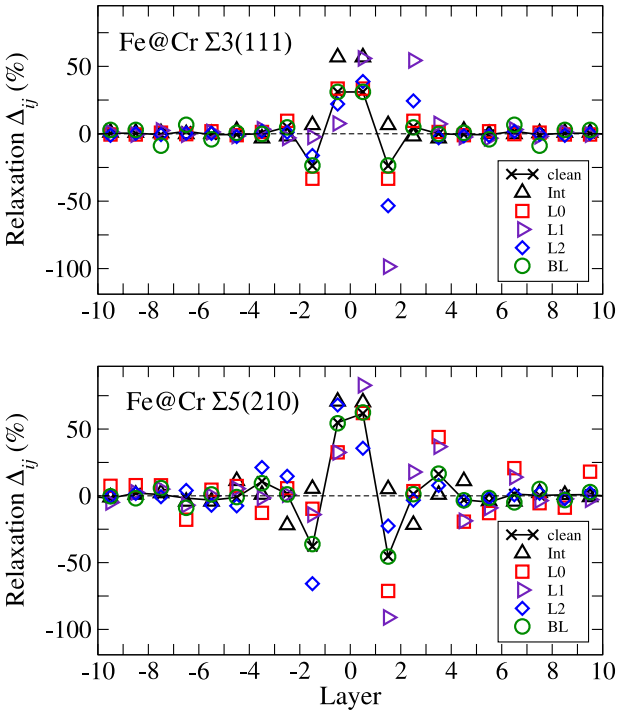

Figure 2. Relaxations of the interplanar spacing in the Cr grains near the boundary. The effect of the solute Fe atoms placed in the GB interstice (Int) or in the substitutional sites of different layers (L) is also shown. BL labels the bulk Cr layer. The (111) and (210) interplanar distances in the bulk truncated Cr are 0.820 and 0.635 Å, respectively.

3. Results and discussion

3.1. Grain boundaries in pure Cr

Figure 2 displays the calculated relaxations of the interplanar distance, $\Delta_{ij} = (d_{ij} - d)/d$, between two subsequent atomic layers, d_{ij}, with respect to their distance d in the bulk truncated crystal. In the grains forming the Σ3 GB the maximum relaxation achieves ∼30%, while at Σ5(210) it can be enhanced even up to ≃60%. The latter is roughly four times larger than that calculated for the free Cr(210) surface [20], where the first three distances are contracted. For the GBs the corresponding distances between layers adjacent to the boundary change in an oscillatory way following the $+ - + +$ pattern, where the '+' and − denote expansion and contraction, respectively. The relaxation of the system does not cause any parallel shift of the Σ3 GB. A very small shift (≃0.02 Å) of the grains parallel to the Σ5(210) boundary plane produces a slightly asymmetric relaxation pattern. The calculated optimum separation between the clean Cr grains is equal to 0.20 Å for the Σ3(111), and is larger (0.35 Å) at the Σ5(210) boundary. The relaxation patterns and their magnitude are similar to those discussed by us for GBs in Fe [21].

The presence of GBs weakens the cohesion in Cr. The calculated cohesive binding energy in the Cr crystal with Σ3 and Σ5 GBs (the enthalpy of GB formation) is respectively 4.12 and 4.07 eV/atom, compared to 4.21 eV/atom for a

Table 1. Calculated GB energy, γ_{gb}, and the formation energy, γ_f, for the pure $\Sigma3(111)$ and $\Sigma5(210)$ GBs in chromium.

	$\Sigma3(111)$		$\Sigma5(210)$	
Boundary	(eV)	(J m^{-2})	(eV)	(J m^{-2})
γ_{gb}	1.63	1.88	2.80	2.52
γ_f	−4.09	−4.71	−4.55	−4.09

perfect AFM Cr crystal. Thus the average binding is 0.05–0.07 eV/atom weaker when GBs are present. The GB energies presented in table 1 show that γ_{gb} of the $\Sigma3(111)$ is smaller than that of the $\Sigma5(210)$ GB. Unfortunately, there are no experimental data to compare with. However, the ratio of the $\Sigma5(210)$ GB energy to the calculated surface energy (per unit area) of the Cr(210) facet [20] is 0.74, which agrees with the well-known trend [13]. This energy ratio, and more generally, the trends in cohesive properties of GBs in chromium are similar to those reported by us for iron [21], the respective energetic values being higher for chromium. The calculated γ_f for the clean GBs are presented in table 1. The formation of the $\Sigma3(111)$ boundary costs 0.62 J m^{-2} more energy than that of $\Sigma5(210)$. The latter is less stable because at the $\Sigma5(210)$ GB only one in five lattice sites coincides, i.e., compared with the $\Sigma3(111)$ there are fewer bonds to break. A lower stability of $\Sigma5(210)$ is manifested by much larger relaxations of atomic layer positions (figure 2). The ratio of the formation energy of the $\Sigma5$ GB to the surface energy of the (210) facet is very similar for Cr (1.28) and Fe (1.31). This ratio informs about the departure, of two surfaces in contact, from perfect registry (cf (2)).

The variations in the local magnetic moments on Cr atoms (m_{Cr}) near GBs are plotted in figure 3. In the grain interior the moments are in the range of 0.30–0.35 μ_B, and thus they are about two times lower than in the bulk Cr crystal (0.59 μ_B [20]). The m_{Cr} on atoms belonging to even and odd layers are aligned antiparallel. Their variation with the layer depth (counted from the boundary plane) is monotonic towards the bulk. For the $\Sigma3$ GB the moment on even-layer atoms is enhanced to 0.6 μ_B at the boundary (zeroth) layer, it decreases to 0.25 μ_B on the second-layer atom, to approach monotonically 0.30 μ_B in deeper layers. For the odd layers the m_{Cr} is lowest at the boundary layer (−0.2 μ_B) and increases to −0.3 μ_B going to deeper layers. At the $\Sigma5$ GB the variation in m_{Cr} is quite similar to $\Sigma3(111)$, except of the boundary layer (L0) atoms where m_{Cr} is much lower than for the $\Sigma3(111)$. The m_{Cr} is smallest (∼0.10–0.15 μ_B) at the odd layer, and largest at even-layer atoms, closest to the boundary. The m_{Cr} on atoms near the $\Sigma5(210)$ GB is about halved compared to that in bulk chromium, and is increased again to 2/3 of the value of m_{Cr} in the ideal chromium crystal, for layers more distant from the GB. This behaviour differs completely from that for the free Cr(210) surface [20], where the $m_{Cr} \simeq 1.8$ μ_B on surface layer atoms, i.e., it is tripled compared to the bulk. The magnetic configuration across the GB slab (figure 3) resembles that of the incommensurate spin density waves structure reported for pure chromium bulk [32], and the amplitude of the calculated m_{Cr} is similar to that observed for Fe/Cr(001) multilayers [33], represented by thick

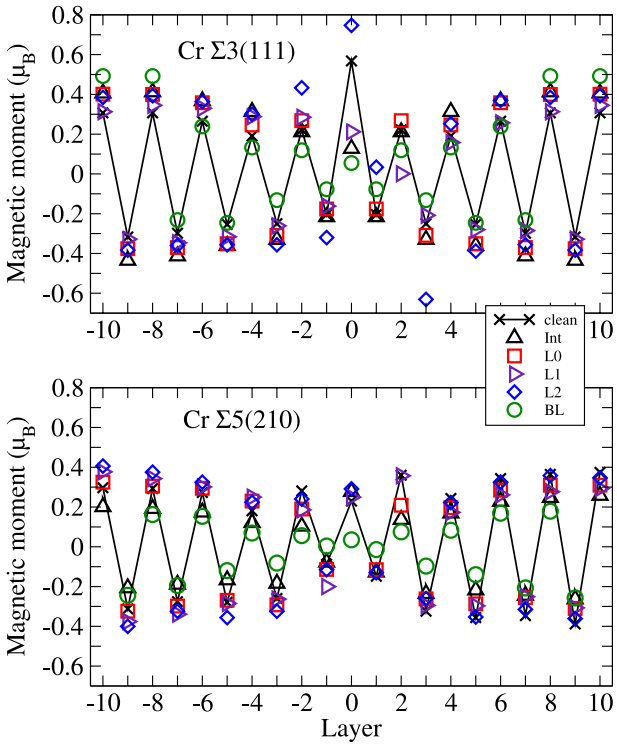

Figure 3. Magnetic moments on Cr atoms of various layers of the grains (cf figure 1) in the vicinity of the clean GB and the boundary doped with Fe atoms.

slabs of Cr atoms separated by a few layers of Fe atoms, where the m_{Cr} was reported to be below 0.5 μ_B.

3.2. *Fe impurities at Cr grain boundaries*

Two different iron concentrations were examined at each GB: by placing one Fe atom in the GB cell we considered a monolayer and a quarter of monolayer of Fe in 1 × 1 and 2 × 2 supercells for $\Sigma3$ GB, and a monolayer and a half a monolayer in 1 × 1 and 1 × 2 cells at $\Sigma5$ GB. Throughout this work a monolayer and fraction of a monolayer of Fe solute atoms are referred to as high and low (planar) Fe concentration, respectively. Note that in all considered cases, the volume concentration of Fe atoms is very small (below 6%).

3.2.1. Geometry and cohesion. The atomic radii of Fe and Cr are alike, and Fe additions substituted to the Cr matrix do not cause any misfit and should not introduce any meaningful strain to the host structure. In figure 2 we show the changes in interlayer relaxations caused by a monolayer of Fe substituting different Cr layers. For clarity only the effect of Fe placed in the layers adjacent to the boundary is shown. As can be seen, an Fe atom placed either in the GB interstice or in substitutional positions may substantially alter the magnitude of relaxation of the Cr atomic planes but the qualitative character of changes remains the same as for the pure Cr GB. The changes in relaxation of chromium planes are most pronounced in the neighbourhood of the Fe impurity. For Fe substituted in one of the layers close to the GB, the relaxation

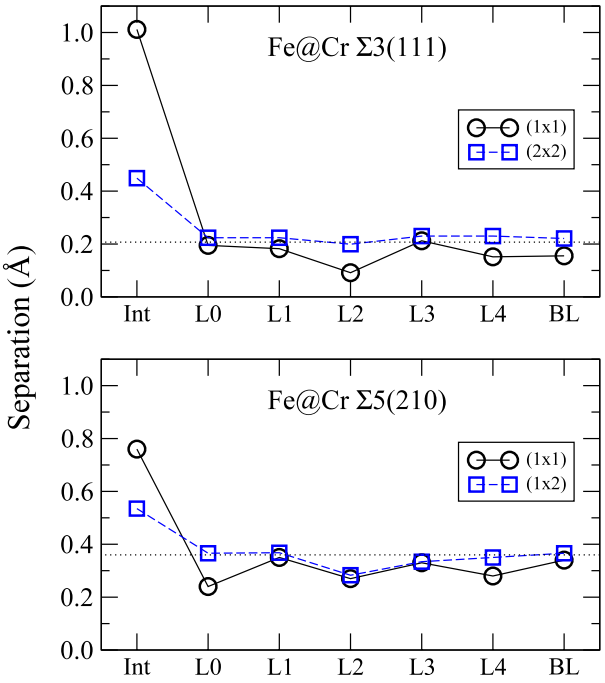

Figure 4. Change in the Cr grain separation due to Fe impurities placed in different positions at the boundary in Cr. The horizontal, dotted line marks the value for pure grains. BL labels the bulk (central) layer of the grain (L10 and L9 for Σ3 and Σ5, respectively).

is more than doubled compared to that observed at the pure Σ3 GB, and nearly doubled at the Σ5 GB. The relaxation enhancement caused by the interstitial Fe is large at the GB plane and rather moderate for the deeper layers. The effect of additions is much weaker for the lower Fe concentrations, in particular at the Cr Σ3 GB.

In figure 4 we have plotted the changes in separation of Cr grains due to Fe atoms. It is seen that only Fe atoms placed in the interstice between the Cr grains increase their separation. This increase is largest for a monolayer of Fe and is connected with the formation of a new Fe layer by atoms placed originally in the interstitial sites at the GB. Fe atoms placed in the GB interstice do not produce any parallel shift of the grains. Substitutional Fe either does not alter or reduces the grains separation compared to clean GBs. Also it does not cause any grains shift parallel to the Σ3(111) boundary plane, whereas at the Σ5(210) a very small shift that is observed at the clean GB, is much enhanced when a monolayer of Fe is placed substitutionally. The size of this shift depends on the position of the Fe monolayer: it is largest (0.7 Å) for Fe in the boundary plane (L0), and smallest (0.06 Å) for Fe in the bulk (BL).

The effect of Fe additions on the cohesive energy of GBs is displayed in figure 5. At the lower concentration, Fe does not change the cohesive bonding at the Σ3 GB in Cr (left panel). At higher concentration Fe atoms can act both as a cohesion enhancer or embrittler, depending on their location, though the strengthening effect of Fe additions is rather weak compared to that of a Cr atom at Fe GBs [21], even for interstitial Fe. For a monolayer of Fe, the strengthening effect is determined by the mechanical energy component (figure 5). A much larger strengthening effect of interstitial Fe at the Σ5 GB than at the Σ3 is connected with differences in the geometry of these systems. An Fe atom placed in the Σ3(111) GB interstice binds only with two atoms—each of a different grain, while at the Σ5(210) it binds with four atoms (two per grain). It results in the formation of four additional bonds between grains at the Σ5 boundary and only in two bonds at the Σ3 GB. For a lower Fe contents all components are small and nearly exactly cancel each other.

At the Cr Σ5 GB substitutional Fe atoms have no significant effect on the cohesion. The ingredients of the strengthening energy cancel almost exactly (figure 5, right panel), even when the individual energies are of 1–2 eV. The effect of the interstitial Fe is boundary specific. While at the Σ3 GB interstice Fe is rather neutral or embrittling, at the Σ5(210) Fe clearly strengthens the boundary (figure 5, right panel), at both concentrations, though it is almost halved at the lower solute concentration. For lower concentration (larger cell) we found two stable interstitial sites for Fe atom placement at the Σ5 GB (cf figure 1). An Fe impurity placed in the `b` site enhances cohesion at GB, whereas that located in the `a` site acts as an embrittler. However, comparison of the total energies shows that the latter configuration is by about 4 eV less favourable. The strengthening effect of interstitial Fe at Σ5 GB is dominated by the chemical contribution. The chemical binding energy differences induced by the presence of Cr at the GB result from the electron charge transfer between Fe and neighbour Cr. By applying the Bader [34, 35] method to calculate charges on atoms at the GBs, we found that consistently with the electronegativity difference between Fe and Cr, the charge is transferred from Cr to Fe. For a lower areal concentration of Fe, the number of electrons on the Fe atom at the Σ5(210) interstice is increased by about 1.5e. The charge is donated by neighbouring Cr atoms. Judging from the data of figure 5 this charge transfer contributes to the strengthening of the Σ5(210). The charge acquired by the interstitial Fe at the Σ5(210) GB is larger than that on the Fe at Σ3(111) interstice. In the latter case two Cr atoms nearest to the Fe (each of different grain) also gain a small amount of charge. The situation is reversed when the Fe atom is placed in the L0 layer. In this case more charge is transferred to the Fe at Σ3 GB than at Σ5. In the two cases, however, the charge gain is smaller than that on the Fe atom in the bulk Cr layer (BL). For Fe atoms situated at layer L2, or deeper inside the grains, the charge transfer to the impurity atom is stabilized at the bulk value of about 0.7e. More quantitative conclusions about charge transfer would require many more detailed calculations for all reconstructed systems and be beyond the scope of this work.

The strengthening effect correlates with a much reduced (almost to zero) magnetic moment on Fe atoms in the interstice and substitutional L1 places. This very small magnetic moment on Fe atoms is, in turn, related to the reduced distances to their nearest neighbours ($\lesssim$2.3 Å), which are by about 7% smaller than in an ideal Cr crystal. The two configurations of the system, one with an Fe atom in the GB interstice, and the other with Fe in the L1 site, are very similar. In both cases a

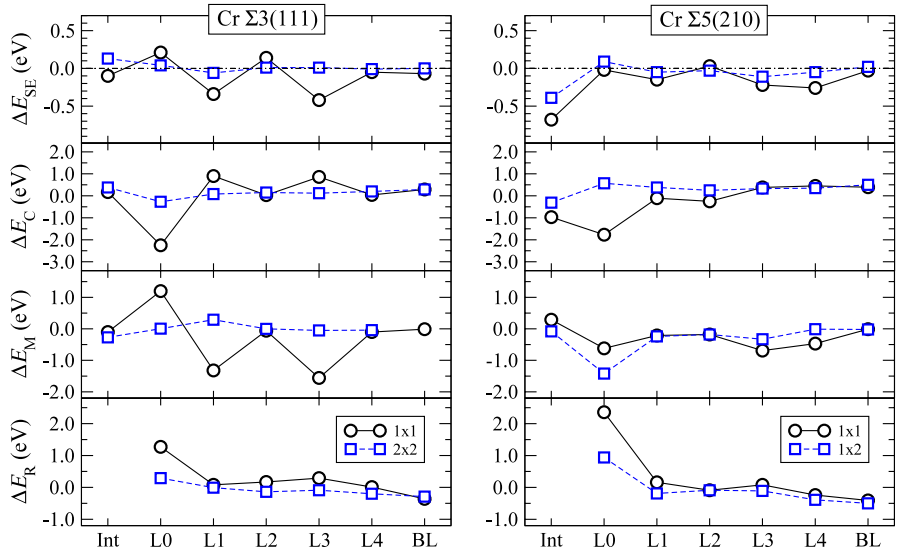

Figure 5. Strengthening energy (top panel) and its chemical, mechanical, and host removal energy components for GBs in chromium doped with Fe placed either in the boundary interstice or in substitutional positions across the GB slab. The horizontal line in the uppermost panels marks the energy zero.

monolayer of FeCr alloy is formed. In the first case, a FeCr monolayer is formed when iron is placed in the GB interstice and it remains stable during relaxation. For Fe substituted in the L1, the configuration results from a relaxation of the system: the L2 and L1 layers of Cr and Fe atoms, respectively, are moved closer to each other to create a mixed FeCr layer. This is clearly visible from the relaxation pattern (figure 2) where, at both GBs, the distances between the first and second layer are reduced by more than 90%. Finally, it is worth mentioning that the strengthening of Cr GBs by Fe additions is much weaker than that caused by interstitial Cr at GBs in iron [21].

3.2.2. Fe segregation at Cr GBs. The surface energy of a free Fe facet is lower than that of a pure Cr, thus according to simple thermodynamic criterion, Fe should segregate at the free Cr surface. This rule is not always obeyed in the FeCr systems (cf [36] and references therein). In order to verify if this argument holds at Cr interfaces, we calculated the energy of segregation of Fe solute in different layers of Cr grains (equation (4)). As is seen from figure 6, the energy of segregation is negative when Fe is substituted for Cr in the interface layers, which means that Fe enriches the GB. Note that atoms in the L0, L1, L2 layers at Σ3(111) GB, and atoms of the zeroth to fourth layer at Σ5(210) GB belong to the boundary atoms, because their coordination is lower than that in the bulk layers (figure 1), and their environment is partly determined by the atoms of the other grain. Thus, the segregation of Fe is favourable down to the third and fourth subsurface layer of the (111) and (210) oriented Cr grains, i.e., down to the layers which are exposed at the respective free surfaces, and depends relatively little on the Fe concentration. It is worth noting that the energy of segregation of Fe at Cr GBs is much higher than that of Cr segregating to GBs in Fe [21].

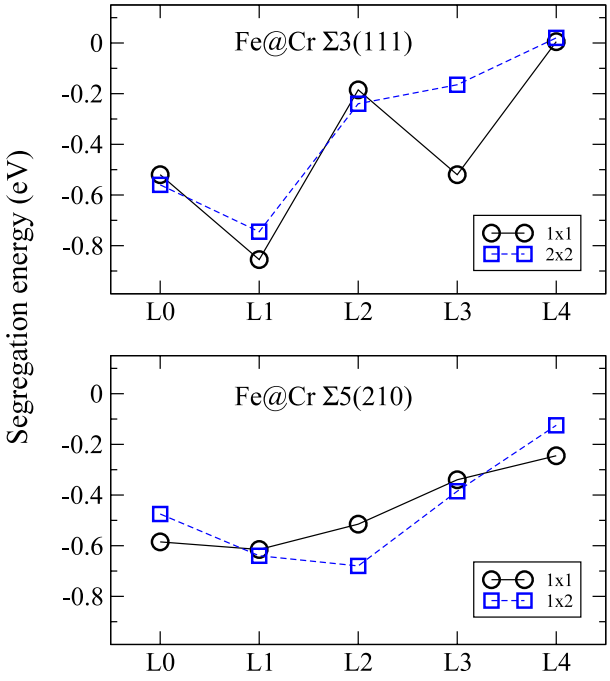

Figure 6. Energy of segregation of Fe solute in different layers at the Σ3 and Σ5 boundaries in chromium for two different Fe areal concentrations (cf text).

3.2.3. Magnetic properties. The variations in the magnetic moments on Cr-host atoms due to a presence of the Fe additions are plotted in figure 3. The values of the m_{Cr} are of similar magnitude or altered by 20–30% in comparison to those for clean GB, and typically attain the values of 0.3–0.4 μ_B, i.e., smaller than for chromium bulk (0.59 μ_B). For Fe additions placed substitutionally in the bulk layer (BL) the moments on Cr-host atoms are systematically reduced in the layers closer to the interface, and the magnetism is almost

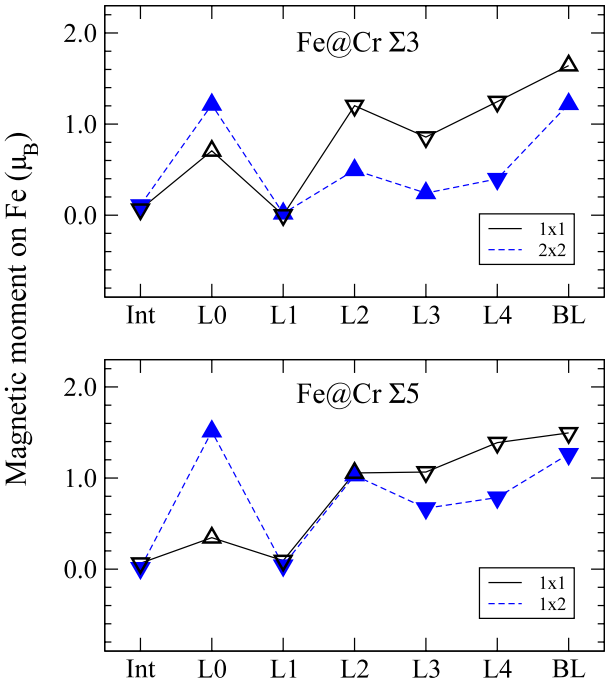

Figure 7. Absolute values of the magnetic moment on an Fe impurity atom placed interstitially or substitutionally in different layers at two different boundaries in Cr. For each concentration, triangles up and down show the direction of the moment.

completely frustrated at the GB layer (L0) as well as in the first sublayer (L1). For the Σ5 GB the effect of Fe solute is slightly asymmetric with respect to the GB plane because of the small shift of the grains. Interstitial Fe atoms suppress the moments m_{Cr} when going from the bulk Cr to the interface layers.

The variations in the magnetic moment on Fe additions are presented in figure 7. In all cases the absolute magnetic moment on Fe atom (m_{Fe}) is greatly reduced or frustrated compared to the value characteristic for bulk iron (2.24 μ_B). The frustration of the m_{Fe} in the GB interstice and L1 positions is connected with the reduced distance between the Fe atom and its nearest Cr neighbours (2.16 Å at Σ3 GB, and 2.30 or 2.05 Å for Fe in the Int or L1 sites at Σ5). The $|m_{Fe}|$ on atoms placed in the L0, L2, L3, L4, and bulk layers, is increased to about 1.0–1.5 μ_B, and thus exceeds that on the bulk Cr atom. The distance of Fe positioned in these sites, to its nearest neighbours, is relatively large (2.35–2.55 Å) and not much different from that in the bulk layers (2.46 Å). The moment on an Fe atom placed in a bulk layer of the grains is equal to about 1.5 μ_B, i.e., is only two-third of that characteristic for the bulk iron.

An analysis of the directions of the magnetic moment on the Fe impurity and on the Cr-host atoms shows that in bulk layers, the moments on Fe atoms and those on their nearest Cr neighbours are parallel, regardless of the concentration and the GB type. However, when placed at the boundary site, the m_{Fe} try to align antiparallel to their NNs. At lower concentration (larger cells), when Cr and Fe atoms are in the same plane, the moments on Fe atoms in bulk sites are antiparallel to those on Cr atoms of the same GB layer. This is a consequence of the ferromagnetism of iron. In AFM chromium, all NNs of Fe atom are in the neighbouring Cr planes (normal to the GB plane) and their magnetic moments are antiparallel to those on Cr atoms in the GB plane which contains Fe impurity. In case of the Σ3 GB, the above described magnetic configuration appears already when Fe is in the L2 layer. For the Σ5(210) such a configuration starts with Fe at the fourth layer (L4). This is not surprising because in the (210) oriented bcc slab, bulk coordination is attained by atoms of deeper layers than at bcc(111).

For Fe in GB layers the perturbed magnetic configuration depends both on the local geometry and the atomic environment. The magnetic moment on an Fe atom is frustrated when it cannot be parallel to that on its NNs, which takes place when Fe is in Int and L1 positions. More generally, we can say that the m_{Fe} on an Fe atom placed in a deeper layer is parallel to its NNs. At the boundary layers, where the geometry is much more changed, the magnetism on Cr-host atoms is decisive and the moments on Fe atoms are antiparallel to those on their nearest Cr neighbours, but the magnitude of m_{Fe} is very small (close to zero).

Our results for the BL configuration show a similar trend of the values of m_{Fe} as those of other calculations performed for different Fe concentrations in FeCr alloys [2, 6, 7]: the m_{Fe} is lower than in an ideal Fe crystal, but much higher than that on Cr atoms. At the 20% of Fe concentration in FeCr alloy, the m_{Fe} was reported [2] in the range of 0.9–1.8 μ_B, whereas the moment on Cr was below 0.2 μ_B. Antropov *et al* [6] reported 2.17 or −1.83 μ_B on Fe and 0.59 μ_B on Cr atoms. For a lower concentration of Fe (≃6%) in a bulk FeCr alloy, the m_{Fe} was reported [7] to be equal 1.81 μ_B or −0.61 μ_B, and ±(0.9–1.0) μ_B on its Cr NNs. Much more reduced moments for Fe (≃0.2 μ_B, which is lower than that on host atoms), and much enhanced moments for Cr (≃ ± 1.2 μ_B) were recently reported [8, 9] for a very low Fe concentration (<2%). One can conclude that for a low volume Fe concentration the magnetic moment on the host atoms is not much altered, whereas the moment on Fe additions is substantially reduced. For higher Fe concentration, the moment on Fe atoms is much larger than m_{Cr}, but is still below the value in bulk Fe crystal. Some part of the difference in the values of m_{Cr} calculated in this work and by other authors [2, 6–9] originates from the different lattice parameter applied, which in all works cited above was larger than ours by about 0.02–0.04 Å. This small increase in the lattice parameter gives a large increase in the calculated m_{Cr} of the ideal Cr crystal. For a lattice constant applied by us, 2.841 Å, changed to 2.86 and to 2.88 Å, the m_{Cr} is increased respectively, from 0.59 to 0.78 μ_B, and to 0.94 μ_B, without changing the AFM behaviour of the system.

4. Summary

The properties of GBs in pure chromium and the effect of a small concentration of Fe additions on the structural, cohesive, and magnetic properties of GBs in Cr was investigated from first principles. For the two high-angle tilt boundaries studied: Σ3(111) and Σ5(210) we found very large enhancement of the interplanar distance in the vicinity of GBs in pure Cr grains. The Fe additions alter the relaxations, but the qualitative

character of changes in the interplanar distance remains similar to that for GBs in pure Cr. A very small parallel shift of the grains observed for the pure Σ5(210) is much increased when Fe additions are inserted substitutionally, whereas for Σ3 GB no such shift is observed. Fe atoms placed in the GB interstice enhance greatly the grains separation. The effect of substitutional Fe on the grains separation is small. The formation of the clean Σ3(111) GB costs 15% more energy per area unit than that of the Σ5(210). A monolayer of iron acts either as a cohesion enhancer or a weak embrittler at Σ3, depending on the place where Fe is located. Small concentrations of Fe additions do not cause strengthening of Σ3 GB. At the Σ5 GB, interstitial iron clearly strengthens the boundary both for the high and a lower Fe concentration. At lower concentration substitutional Fe solutes are weak enhancers or have no effect on the cohesion. We have found that the boundaries in Cr enriched with Fe atoms are favourable by several tenths of eV, in comparison to those containing Fe in the Cr grains interior. The magnetic structure of the considered GBs resembles that of incommensurate spin density waves, which is characteristic of the AFM chromium crystal, however, with the amplitude of the magnetic moment on Cr atoms substantially reduced. Fe additions have only a small effect on the magnetic configuration of the grains, and the greatest changes in the magnetic moment of the host atoms are observed near the impurity.

Acknowledgments

We appreciate useful discussions with Professor K J Kurzydłowski on GB properties. This work was supported by the Ministry of Science and Higher Education (Poland) under Grant No. COST/201/2006. We acknowledge allocation of computer time by the Interdisciplinary Centre for Mathematical and Computational Modeling (ICM), University of Warsaw (Grant G28-25).

References

[1] Cote P J and Rickard C 2005 *Wear* **241** 17
[2] Klaver T P C, Drautz R and Finnis M W 2006 *Phys. Rev.* B **74** 094435
[3] Olsson P, Abrikosov I A and Wallenius J 2006 *Phys. Rev.* B **73** 104416
[4] Olsson P, Domain C and Wallenius J 2007 *Phys. Rev.* B **75** 014110
[5] Klaver T P C, Olsson P and Finnis M W 2007 *Phys. Rev.* B **76** 214110
[6] Antropov V P, Anisimov V I, Liechtenstein A I and Postnikov A V 1988 *Phys. Rev.* B **37** 5603
[7] Hashemifar S J, Ghaderi N, Sirousi S and Akbarzadeh H 2006 *Phys. Rev.* B **73** 165111
[8] Mishra D N 2008 *Phys. Rev.* B **77** 224402
[9] Mishra S N and Srivastava S K 2008 *J. Phys.: Condens. Matter* **20** 285204
[10] Krasko G L and Olson G B 1990 *Solid State Commun.* **76** 247
[11] Geng W T, Freeman A J, Wu R and Olson G B 2000 *Phys. Rev.* B **62** 6208
[12] Geng W T, Freeman A J and Olson G B 2001 *Phys. Rev.* B **63** 165415
[13] Yamaguchi M, Shiga M and Kaburaki H 2006 *Mater. Trans. JIM* **47** 2682
[14] Yamaguchi M, Nishiyama Y and Kaburaki H 2007 *Phys. Rev.* B **76** 035418
[15] Braithwaite J S and Rez P 2005 *Acta Mater.* **53** 2715
[16] Wachowicz E and Kiejna A 2008 *Comput. Mater. Sci.* **43** 736
[17] Čák M, Šob M and Hafner J 2008 *Phys. Rev.* B **78** 054418
[18] Ostroukhov A A, Floka V M and Cherepin V T 1995 *Surf. Sci.* **331–333** 1388
[19] Kolesnychenko O Yu, Heijnen G M M, Zhuravlev A K, de Kort R, Katsnelson M I, Lichtenstein A I and van Kempen H 2005 *Phys. Rev.* B **72** 085456
[20] Ossowski T and Kiejna A 2008 *Surf. Sci.* **602** 517
[21] Wachowicz E, Ossowski T and Kiejna A 2009 arXiv:0903.1618v2 [cond-mat.mtrl-sci]
[22] Perdew J P, Chevary J A, Vosko S H, Jackson K A, Pederson M R, Singh D J and Fiolhais C 1992 *Phys. Rev.* B **46** 6671
[23] Kresse G and Hafner J 1993 *Phys. Rev.* B **47** R558
Kresse G and Hafner J 1994 *Phys. Rev.* B **49** 14251
[24] Kresse G and Furthmüller J 1996 *Phys. Rev.* B **54** 11169
Kresse G and Furthmüller J 1996 *Comput. Mater. Sci.* **6** 15
[25] Blöchl P 1994 *Phys. Rev.* B **50** 17953
[26] Kresse G and Joubert D 1999 *Phys. Rev.* B **59** 1758
[27] Sutton A P and Balluffi R W 1995 *Interfaces in Crystalline Solids* (Oxford: Clarendon)
[28] Monkhorst H J and Pack J D 1976 *Phys. Rev.* B **13** 5188
[29] Methfessel M and Paxton A 1989 *Phys. Rev.* B **40** 3616
[30] Rice J R and Wang J-S 1989 *Mater. Sci. Eng.* A **107** 23
[31] Lozovoi A Y, Paxton A T and Finnis M W 2006 *Phys. Rev.* B **74** 155416
[32] Zabel H 1999 *J. Phys.: Condens. Matter* **11** 9303
[33] Amitouche F, Issolah A, Bouarab S, Vega A and Demangeat C 2009 *Surf. Sci.* **603** 117
[34] Bader R F W 1990 *Atoms in Molecules: a Quantum Theory* (Oxford: Oxford University Press)
[35] Henkelman G, Arnaldsson A and Jónsson H 2006 *Comput. Mater. Sci.* **36** 354
[36] Kiejna A and Wachowicz E 2008 *Phys. Rev.* B **78** 113403